Analysis of the energy transport and deposition within the reaction chamber of the Prometheus inertial fusion energy reactor

J.E. Eggleston, M.A. Abdou, M.S. Tillack

Mechanical, Aerospace and Nuclear Engineering Department, University of California, Los Angeles, CA 90024-1597, USA

Abstract

The thermodynamic response of the Prometheus reactor chamber was analyzed and, from this analysis, a simplified thermodynamic response model was developed for parametric studies on this conceptual reactor design. This paper discusses the thermodynamic response of the cavity gas and models the condensation/evaporation of vapor to and from the first wall. Models of X-ray attenuation and ion slowing down are used to estimate the fraction of the pellet energy that is absorbed in the vapor. It was found that the gas absorbs enough energy to become partially ionized. To treat this problem, methods developed by Zel'dovich and Raizer are used in modeling the internal energy and the radiative heat flux of the vapor.

From this analysis, RECON was developed, which runs with a relatively short computational time, yet retains enough accuracy for conceptual reactor design calculations. The code was used to determine whether the reactor designs could meet the stringent mass density limits that are placed on them by the physics of beam propagation through matter. RECON was also used to study the effect that the formation of a local dry spot would have on the first wall of the reactor. It was found that, for a typical reactor lifetime of 30 years, the first wall could not have a dry spot over any one section for more than 15.5 min for the laser driver design and 4.5 min for the heavy ion driver design. These times are relatively short, which implies that there is a need to keep the liquid film attached at all times.

1. Introduction

One of the most serious problems with inertial fusion energy (IFE) reactors is the design of a reaction chamber that can withstand the intense heat fluxes that are inherent in IFE and can also keep the cavity vapor density low enough to allow proper irradiation of the target by the laser or heavy ion beams. As part of the Prometheus reactor study [1], a detailed thermal analysis of the reactor chamber was carried out [2]. This led to the proposed reactor design that uses a thin liquid metal lead film to protect the reactor's first wall (FW) from the direct X-ray energy deposition and the heat flux emanating from the hot vapor in the reaction chamber. The liquid metal film will partially evaporate under the intense energy flux, but after it cools it will begin to recondense back onto the walls. This makes it necessary to analyze the full thermal response of the reactor to verify whether the vapor density falls below the limits for reactor operation fast enough to satisfy the repetition rate requirement of 5–10 Hz.

This paper clarifies and analyzes the different processes that are important in formulating the thermal response model to be used in a simplified computer code. This code analyzes the thermodynamic response of a given IFE reactor without trying to solve for the hydrodynamic response. Much more sophisticated codes have been developed for this, such as CONRAD developed at the University of Wisconsin [3]; however, these codes were not available for parametric studies.

Once a knowledge of the reactor's thermal response is obtained, the ability of the reactor to meet the stringent requirements placed on it by the physics can be determined. Also, with this information, the reactor's response to the formation of a local dry spot on the FW can be investigated. The radiative heat flux calculated by the thermal response model is used to analyze the sublimation rate of SiC in the reactor's FW. This information is important in determining the lifetime of the FW component and providing an indication of the feasibility of the reactor design.

2. Heat and mass transfer in the IFE cavity

2.1. Energy deposition

In Prometheus, the X-rays produced in the pellet explosion must pass through the lead vapor that fills the cavity. Since lead is a high Z material, it is a very efficient photon attenuator and as such will absorb a portion of the X-rays before they reach the FW. The fraction of X-rays that reaches the FW is absorbed by the lead film. As the liquid lead absorbs the X-ray energy, some of the lead will evaporate to a depth x_1, which can be calculated by noting to what depth the bulk heating q is greater than the latent heat of evaporation ρh_{fg} of the liquid lead; x_2 is the depth at which q equals $\rho C_p \Delta T$, which is the energy needed to bring the lead just to the boiling point. In between x_1 and x_2 is a two-phase region that contributes to the total depth of evaporation. The contribution of the two-phase region can be estimated by assuming that the liquid which is vaporized is just equal to the amount that is energetically favorable. This treatment does not allow for droplet formation nor for anomalies in the local energy content of the film. This is an average treatment in which the film maintains its integrity. The total evaporation depth δ can then be estimated as

$$\delta = x_1 + \frac{\int_{x_1}^{x_2} (q_{evap} - \rho C_p \Delta T) \, dx}{\rho h_{fg}} \tag{1}$$

From this the evaporated mass is determined by $M_{evap} = \rho A \delta$.

Most of the ionized target debris is stopped before reaching the liquid surface. The ion energy deposition can be calculated by integrating the ion stopping power, $-dE/dx$, over the distance the ion travels. Semi-empirical formulae proposed by Anderson and Ziegler [4] and Ziegler [5] for hydrogen and helium in lead were used in the model to calculate the stopping power of the target debris. The results of the equations can be extrapolated for other particles, i.e. deuterium, tritium, carbon and lead. The extrapolation is carried out by noting that the stopping power at high energies is proportional to Z^2 and inversely proportional to the mass of the particle [6]. Thus, if the stopping power of one kind of particle is known, the stopping power of a second type can easily be solved. For low-energy ions, this type of extrapolation is not valid, since at low energies the ions undergo complicated interactions with the absorbing material making the stopping power differ from the simple Z^2 dependence. However, at low energy, the ions do not contribute much to the heating of the vapor and the extrapolation can be used to estimate the energy deposition of the ions in the vapor.

To use the stopping power equations, the initial ion spectrum must be determined. This is calculated by treating the particles as a "single fluid" as they explode away from the pellet, i.e. all the debris is treated as moving with a uniform velocity. Since all the particles have the same velocity $\bar{U}$, the individual particle initial energies can be solved by

$$E_i = \frac{M_i}{M_T} E_T \tag{2}$$

The ion energy spectra in Table 1 were based on debris energies of 107 MJ for the laser and 159 MJ for the heavy ion targets.

2.2. Thermal response model

There are different energy transport pathways that need to be modeled in a pellet explosion: thermal radiation from the vapor, evaporation/condensation of the lead film and conduction through the FW. The modeling of these different pathways is depicted in Fig. 1 and discussed below.

2.2.1. Determination of the temperature of a partially ionized gas

Since both the mass of vapor and the energy deposited in the vapor are known, the specific energy of

Table 1
Target debris ion masses, numbers and energy per ion

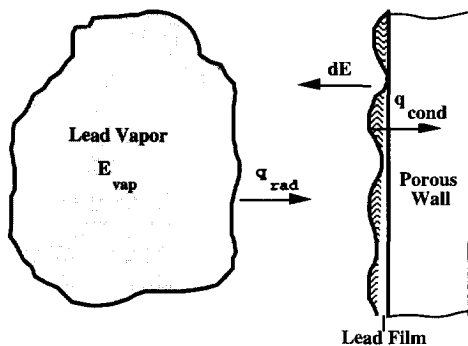| Ion	Laser driver			Heavy ion driver		
	M_i (mg)	Number of ions	E_i (keV)	M_i (mg)	Number of ions	E_i (keV)
D	1.33	4.01×10^{20}	105.39	1.68	5.06×10^{20}	8.06
T	2.0	4.01×10^{20}	158.48	2.52	5.06×10^{20}	12.09
He	1.1	1.72×10^{20}	210.6	1.44	2.17×10^{20}	16.11
C	16.27	8.16×10^{20}	633.56	325	1.63×10^{20}	48.35
H	1.36	8.16×10^{20}	52.95	27.08	1.63×10^{20}	4.03
Pb	0.0	0.0	0.0	7.8	2.27×10^{20}	834.80
Total	21.02		1160.98	409.0		919.40

Fig. 1. Energy transfer within the Prometheus reactor chamber.

the vapor can be calculated. Using this, in conjunction with an analytical equation for the specific energy derived by Zel'dovich and Raizer [7], the temperature of the vapor can be determined. For a given temperature, the specific energy of a gas ε is determined by

$$\varepsilon = \frac{3}{2}(1 + \bar{m})kT + Q(\bar{m}) \tag{3}$$

The charge state $\bar{m}$ is the average ionization state of each atom. Thus the first term is the kinetic energy contained by the $1 + \bar{m}$ particles of a given atom, and $Q(\bar{m})$ is defined as the sum of the ionization potentials needed to ionize the atom to charge state $\bar{m}$

$$Q(\bar{m}) = \sum_{n=1}^{\bar{m}} \bar{I}_n \tag{4}$$

where $\bar{I}_n$ is the average ionization potential for charge state n and can be approximated by the use of equations derived by Zel'dovich and Raizer [7]. The discrete values of $Q(\bar{m})$ can be made continuous by interpolating between them. All that is now needed is the depen-

dence of $\bar{m}$ on temperature. Unfortunately, this involves solving complicated coupled equations with sophisticated codes. To avoid this, the dependence of the charge state on the gas temperature from the LIBRA study [8] was used in this work. Some error is introduced since LIBRA used lithium–lead instead of lead, and lithium is much easier to ionize than lead. However, the average charge should not be that much different since lithium–lead is 83% lead. The presence of the lithium should only perturb the average charge state. Also, at low plasma temperatures, the temperatures of concern in IFE, the charge state has a fairly weak dependence on the density and as such no density dependence is assumed.

2.2.2. Radiative heat flux from a partially ionized gas

Once the temperature and the charge state of the gas are known, the radiative heat flux can be calculated. The vapor is a low-density, low-temperature plasma and as such a modified form of the Stephan–Boltzmann equation, suggested by Zel'dovich and Raizer [7], that takes into account the ionized nature of the gas has been used in the model. They formulated the volumetric cooling rate to be

$$q''' = \frac{4\sigma \Delta T^4}{l_1} \tag{5}$$

where $4\sigma \Delta T^4$ is the standard radiative heat flux from a gray body and l_1 is the average photon mean free path which was derived by Zel'dovich and Raizer and is given in Ref. [7]. It is through l_1 that the ionized nature of the gas is taken into account.

2.2.3. Evaporation and condensation from the FW

The heat flux radiated to the FW will cause the liquid film to evaporate. A simple heat balance across the

liquid film interface is written to calculate the evaporative heat flux, $q_{evap} = q_{rad} - q_{con}$, where q_{rad} is the radiative heat flux from the gas, which is calculated from the volumetric cooling rate, and q_{con} is the heat flux conducted through the film. Knowing q_{evap} makes it possible to calculate the mass flux of lead that is leaving the wall

$$J = \frac{q_{evap}}{h_{fg} + C_p \Delta T} \tag{6}$$

When the surface temperature falls below the saturation temperature of the gas, the vapor will begin to condense onto the surface. However, the condensation process is complicated by the presence of non-condensable gas left over from the fusion process. An equation derived by Pong et al. [9] gives a fairly accurate description of the condensation of a vapor in the presence of a non-condensable gas and was included in the thermal model. With this last piece of information the thermal model is complete. The description of the thermal response of the reactor contains enough engineering accuracy to perform the parametric investigations needed for the Prometheus reactor design study.

With a known mass flux, an energy balance can now be written for the vapor. The vapor energy balance is

$$E_{vap}^{n} = E_{vap}^{o} + dE - q_{rad} A \, dt \tag{7}$$

where $E_{vap}^{n/o}$ is the new or old vapor energy, dE is the incremental energy carried by the lead and $q_{rad} A \, dt$ is the energy radiated from the vapor over the time period dt. The dE term is calculated by $dE = dm c_v (T_{sat/vap} - T_{ref})$, where T_{ref} is the temperature at which the energy of the system is assumed to be zero, which is taken to occur at 0 K, and $T_{sat/vap}$ is the temperature at which the incremental mass is added to the system. For evaporation, the temperature is T_{sat}, i.e. the mass enters the vapor at the saturation temperature of the liquid film, and for condensation the mass leaves the system at the vapor temperature T_{vap}. The incremental mass can be found from the mass flux at the vapor–film interface.

3. Results and discussion

3.1. Energy deposition

The cavity response is strongly dependent on the spectrum of the X-rays that strike the wall. For Prometheus, the SIRIUS [10] spectrum was used for the laser target, and the LIBRA [8] spectrum was used for the heavy ion target. It was found that these were closest to the spectra expected in the Prometheus reactor. For X-ray yields of 31 MJ and 46 MJ in the laser
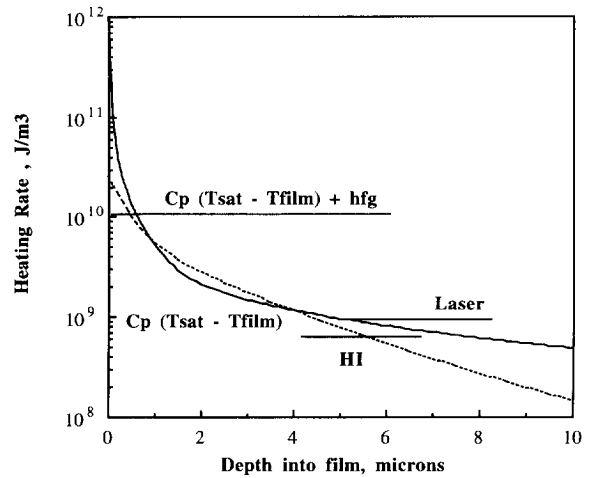

Fig. 2. The volumetric energy deposition profile of the X-rays in the lead film.

and heavy ion designs, it was calculated that the vapor absorbs approximately 80% of the X-ray energy in the heavy ion design and only 30% is absorbed in the laser design. The difference is due to the 100-fold increase in the number density found in the heavy ion design.

Fig. 2 shows the energy deposition curves of X-rays in the liquid metal film. The high vapor density of the heavy ion reactor attenuates much of the low-energy X-rays but does not affect the high-energy ones. This is reflected in the volumetric energy deposition curves in Fig. 2 which clearly show the effects of the vapor pressure and the different X-ray spectra of each driver type. The laser driver with its low vapor pressure shows a much higher, steeper heating rate which is caused by the absorption of the numerous low-energy X-rays that reach the structure. As the X-rays penetrate deeper into the film, the difference in the heating rates reflects the difference in the spectra and is not caused by the vapor density difference.

Eq. (1) is used in conjunction with Fig. 2 to determine the total depth of evaporation δ and the mass evaporated by the X-rays. The analysis shows that 5.9 kg and 6.4 kg of lead are blown from the walls for the laser and heavy ion cases. These masses correspond to total evaporation depths of 1.3 μm and 1.6 μm respectively.

It was found that the particles lose between 90% and 80% of their energy over the first few meters traveled in the vapor [2]. The total fraction of energy lost to the vapor is 85% for the laser reactor and 100% for the heavy ion reactor, which is expected since the ion spectrum for the heavy ion reactor is much softer than that of the laser reactor and the number density for the heavy ion reactor is much greater. However, it is impor-

tant to remember that no attempt has been made to include the time dependence of the film evaporation and the ion deposition processes, i.e. the number density of the vapor will be much larger close to the wall since the vapor has not had time to move from the wall and uniformly fill the cavity. Thus the figure for the laser case represents a lower bound on the energy deposited in the vapor and it can be safely assumed that all the ion energy is deposited in the vapor.

3.2. Thermal response of the IFE reactor chamber

The material properties of the reactor's FW used in RECON are given in Eggleston [2]. The reactor parameters used in the code are given in Table 2. Using these parameters, Fig. 3 was generated giving the vapor mass as a function of time. This represents the volume-averaged thermal response of the reactor; thus no shock waves are calculated here. It should be noted that the important parameter is the vapor mass density. The reactors must reach the density limits of $\rho_{L|HI} = 1.21 \times 10^{-5} |1.21 \times 10^{-3}$ kg m^{-3} before the next pellet is shot. Fig. 3 shows that the vapor mass reaches acceptable limits well within one cycle for both the laser and heavy ion reactors as calculated by RECON. There are a number of approximations that have gone into RECON; they include spherical geometry, no hydrodynamic modeling, the motion of the evaporated film, maintenance of the film with no droplet formation or splashing and the absence of penetrations present in the design.

3.3. Silicon carbide sublimation rate

The porous SiC structure will sublimate under the intense heat flux if left unprotected. The model can be used to study the effect of such a dry spot on the FW
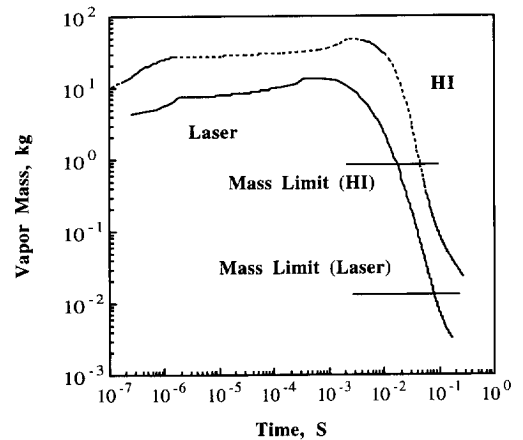

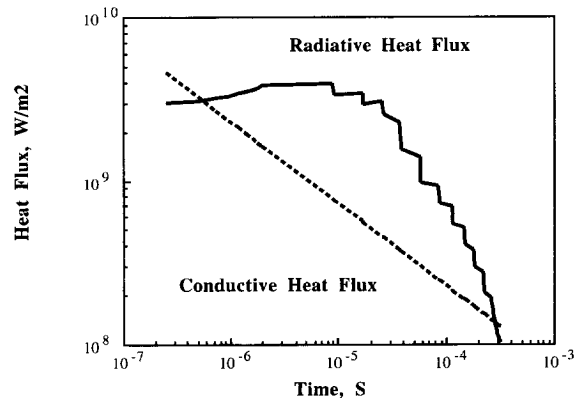Fig. 3. Time evolution of the vapor mass for both the laser and heavy ion reactors.

Fig. 4. Comparison of the radiative flux on and the conductive flux through bare SiC in the Prometheus reactor.

of the reactor. By comparing the radiative heat flux with the flux conducted through the SiC, the amount of SiC sublimated per shot can be determined. Fig. 4 compares these heat fluxes. At intermediate times, the conductive heat flux is less than the radiative flux and the difference between the two is the energy available for sublimation. The sublimation rate per unit area can be calculated by dividing this heat flux by the heat of sublimation, which was found to be 1.91×10^7 J kg^{-1} [2].

The sublimation depth of the bare SiC structure was calculated by integrating the sublimation mass flux over one shot and dividing it by the mass density of SiC. The sublimation depths were estimated to be 9.69 μm for the laser and 54.25 μm for the heavy ions per shot. For

Table 2
Prometheus H/L reactor parameters

Reactor parameter	Heavy ion	Laser	Units
Total pellet yield	719	497	MJ
X-ray yield	46	31	MJ
Ion debris yield	159	107	MJ
Repetition rate	3.6	5.6	Hz
Cavity radius	4.5	5.0	m
Cavity height	4.5	5.0	m
Cavity surface area	382	471	m^2
Cavity volume	668	916	m^2
Non-condensable gas pressure (at 273 K)	1.5	1.5	Pa

an SiC thickness of 5 cm, this rate of sublimation corresponds to burn-through times of approximately 15.35 min and 4.27 min respectively. This analysis does not take into consideration any possible mechanisms of redeposition onto the surface of the liquid lead of any of the sublimated SiC. Also, it was assumed that the dry spot is small enough so as not to affect the overall thermal response of the reactor.

The time to failure is measured in just a few minutes. If a dry spot forms and is maintained for about 15 min for the laser reactor and 5 min for the heavy ion reactor, the FW will be seriously eroded and even breached. This would have serious effects on the design of the reactor, and indicates that the problem of maintaining the film on the surface is of utmost importance. If the reactor design has a problem with sustaining the liquid film over any region of the reactor, there will be major maintenance problems and the reactor design would not be a viable option. Hence any design that is to be implemented must have methods to maintain the film at the critical points within the reactor.

4. Conclusions

The models proposed in this work were used to determine the ability of a reactor design to meet the stringent limits for operation. It was found that the reactor designs were capable of obtaining the vapor density limits within a time period which allows an acceptable repetition rate for power production for the given simplifications of the thermal model. The simplifications include a spherical geometry of the reactor chamber, no hydrodynamic modeling, the time dependence of the lead vapor as it evaporates from the FW, the assumed integrity of the film with no droplet formation or splashing and the absence of penetrations present in the design.

Another area of concern involves the formation of local dry spots on the FW. Using the thermal model developed here, it was found that the structure with a dry spot had a lifetime of only 15.5 min for the laser driver and 4.5 min for the heavy ion driver. These relatively short times raise questions as to the feasibility of the reactor chamber design concept. If a dry spot forms anywhere on the FW, the structure could very well be breached within a relatively short time, forcing a reactor shutdown. It is imperative that the liquid film is attached to the FW and that schemes for the early detection of potential dry spots are used.

Appendix A: Nomenclature

A	surface area of FW
E_i	energy of the type "i" ion
E_T	total energy released to the pellet debris
M_i	mass of the type "i" ion
M_T	total pellet mass
q'''	vapor cooling rate
q_{con}	conductive heat flux through FW
q_{evap}	$q_{rad} - q_{con}$
q_{rad}	radiative heat flux from vapor (calculated from q''' by multiplying by the volume/area ratio)
ΔT	temperature difference of either the vapor or the FW
ΔT^4	$T_{vap}^4 - T_{surf}^4$

References

[1] Inertial fusion energy reactor design studies: PROMETHEUS-L PROMETHEUS-H: final report, McDonnell Douglas Aerospace Team, DOE/ER-54101, March, 1993.

[2] J.E. Eggleston, Analysis of the energy transport within the reaction chamber of the Prometheus inertial fusion energy reactor, Masters Thesis, University of California, Los Angeles, 1993.

[3] R.R. Peterson, J.J. MacFarlane and G.A. Moses, CONRAD—a combined hydrodynamic-condensation/vaporization computer code, University of Wisconsin Fusion Technology Institute Rep., UWFDM-670, revised July 1988.

[4] H.H. Anderson and J.F. Ziegler, Hydrogen Stopping Powers and Ranges in All Elements, Pergamon, New York, 1977.

[5] J.F. Ziegler, Helium Stopping Powers and Ranges in All Elements, Pergamon, New York, 1977.

[6] G.F. Knoll, Radiation Detection and Measurement, Wiley, New York, 1979.

[7] Ya.B. Zel'dovich and Yu.P. Raizer, Physics of Shock Waves and High-Temperature Hydrodynamic Phenomena, Vol. 1, Academic Press, New York, 1966.

[8] LIBRA, a conceptual light ion beam fusion conceptual reactor design, University of Wisconsin Fusion Technology Rep., UWFDM-800, FPA-903, KfK-4710, July, 1989.

[9] L. Pong, M.L. Corradini, R.R. Peterson and G.A. Moses, Liquid metal condensation in the cavity of the HIBALL heavy ion fusion reactor, Nucl. Eng. Des./Fusion, 3 (1985) 47-57.

[10] SIRIUS-T: a study of a symmetrically-illuminated inertial confinement fusion tritium production facility. Final report, UWFDM-850, December, 1990.